Synthesis and Characterization of Phosphated Mesoporous Titanium Dioxide with High Photocatalytic Activity

Jimmy C. Yu,*,† Lizhi Zhang,† Zhi Zheng,† and Jincai Zhao‡

Department of Chemistry and Environmental Science Programme, The Chinese University of Hong Kong, Shatin, New Territories, Hong Kong, China, and The Laboratory of Photochemistry, Center for Molecular Science, Institute of Chemistry, The Chinese Academy of Sciences, Beijing 100080, China

Received February 19, 2003. Revised Manuscript Received April 12, 2003

A surfactant-templated approach was used to synthesize phosphated mesoporous titanium dioxide by incorporating phosphorus from phosphoric acid directly into the framework of TiO_2. The resulting materials were characterized by XRD, nitrogen adsorption, TEM, XPS analysis, UV−vis spectroscopy, FT-IR spectroscopy, and isoelectric point measurements. The surface area of phosphated mesoporous TiO_2 exceeded 300 m^2/g after calcination at 400 °C. It was found that the incorporation of phosphorus could stabilize the TiO_2 framework and increase the surface area significantly. This stabilization is attributed to two reasons: the more complete condensation of surface Ti−OH in the as-prepared sample and the inhibition of grain growth of the embedded anatase TiO_2 by the interspersed amorphous titanium phosphate matrix during thermal treatment. Both pure and phosphated mesoporous TiO_2 show significant activities on the oxidation of *n*-pentane. The higher photocatalytic activity of phosphated mesoporous TiO_2 can be explained by the extended band gap energy, large surface area, and the existence of Ti ions in a tetrahedral coordination.

Introduction

Heterogeneous photocatalysis is an emerging technique for water and air purification and remediation.[1] TiO_2 is one of the most widely studied heterogeneous photocatalysts.[2] Unfortunately, the photocatalytic activity of pure titania is not high enough for industrial purposes.[3] Several methods have been reported to improve the photocatalytic efficiency. These include increasing the surface area of TiO_2, generation of defect structures to induce space-charge separation, and modification of the TiO_2 with metal or other semiconductors.[4−7]

Mesoporous TiO_2 is a highly photocatalytically active photocatalyst because it has a high surface-to-volume ratio and offers more active sites for carrying out catalytic reactions.[8,9] Solvent extraction or thermal treatment at low temperature was often used to remove the surfactants used in the preparation of mesoporous TiO_2.[10,11] However, the amorphous and semicrystalline TiO_2 thus prepared have negligible photocatalytic activity.[12] Calcination at high temperature may not be helpful as it causes the collapse of mesoporous framework and loss of surface area due to the facile crystallization of TiO_2 and the subsequent crystal growth.[13] Since the anatase phase has a far higher photocatalytic activity than amorphous and rutile TiO_2, it is still a challenge to synthesize mesoporous TiO_2 containing the anatase phase of high crystallinity and large surface area.[14]

It was reported that the thermal stability and acidity of mesoporous materials could be greatly improved through post-treatment with phosphoric acid.[15−17] The uncondensed surface hydroxyl groups may react with the phosphate ions, leading to complete cross-linking.[15] Moreover, H_3PO_4 can be polymerized to polyphosphoric acid with network structure at high temperatures. This network structure, which is tightly attached to the surface of mesoporous materials, can effectively resist the shrinkage of pore channels during thermal or hydrothermal treatment.[17] To the best of our knowledge, there is no report on the synthesis of phosphated mesoporous TiO_2 by directly incorporating phosphorus

* To whom correspondence should be addressed. E-mail: jimyu@cuhk.edu.hk. Fax: +852-2603 5057.
† The Chinese University of Hong Kong.
‡ The Chinese Academy of Sciences.

(1) Litter, M. I. *Appl. Catal. B: Environ.* **1999**, *23*, 89.
(2) Yu, J. C.; Lin, J.; Lo, D.; Lam, S. K. *Langmuir* **2000**, *16*, 7304.
(3) Kwon, Y. T.; Song, K. Y.; Lee, W. I.; Choi, G. J.; Do, Y. R. *J. Catal.* **2000**, *191*, 192.
(4) Yu, J. C.; Zhang, L. Z.; Yu, J. G. *New J. Chem.* **2002**, *26*, 416.
(5) Rusu, C. N.; Yates, J. T. *Langmuir* **1997**, *13*, 4311.
(6) Litter, M. I.; Navio, J. A. *J. Photochem. Photobiol. A: Chem.* **1996**, *98*, 171.
(7) Yu, J. C.; Lin, J.; Kwok, R. W. M. *J. Photochem. Photobiol. A: Chem.* **1997**, *111*, 199.
(8) Antonelli, D. M.; Ying, Y. J. *Angew. Chem., Int. Ed. Engl.* **1995**, *34*, 2014.
(9) Ying, Y. J. *AICHE J.* **2000**, *46*, 1902.
(10) Stone, V. F.; Davis, R. J. *Chem. Mater.* **1998**, *10*, 1468.
(11) Yue, Y.; Gao, Z. *Chem. Commun.* **2000**, 1755.
(12) Ohtani, B.; Ogawa, Y.; Nishimoto, S. I. *J. Phys. Chem. B* **1997**, *101*, 3746.
(13) Elder, S. H.; Gao, Y.; Li, X.; Liu, J.; McCready, D. E.; Windisch C. F. *Chem. Mater.* **1998**, *10*, 3140.
(14) Ovenstone, J.; Yanagisawa, K. *Chem. Mater.* **1999**, *11*, 2770.
(15) Ciesla, U.; Schacht, S.; Stucky, G. D.; Unger, K. K.; Schuth, F. *Angew. Chem., Int. Ed. Engl.* **1996**, *35*, 541.
(16) Chen, H. R.; Shi, J. L.; Hua, Z. L.; Ruan, M. L.; Yan, D. S. *Mater. Lett.* **2001**, *51*, 187.
(17) Huang, L. M.; Li, Q. Z. *Chem. Lett.* **1999**, 829.

10.1021/cm0340781 CCC: $25.00
Published on Web 05/09/2003

from H_3PO_4 into the inorganic framework of mesoporous TiO_2. This study shows that direct incorporation of phosphorus from H_3PO_4 can stabilize the framework of mesoporous TiO_2 to produce phosphated mesoporous TiO_2 with high surface area. Moreover, the resulting phosphated mesoporous TiO_2 (PMT) shows very high photocatalytic activity on the oxidation of *n*-pentane in air. In contrast to phosphated mesoporous TiO_2 synthesized with surfactants containing phosphorus as structure templates,[10] photocatalytic activity of PMT is even better than that of pure mesoporous TiO_2 (MT) synthesized by the same procedure.

Experimental Section

Catalyst Preparation and Characterization. The synthesis procedure of phosphated mesoporous TiO_2 was straightforward. Three grams of triblock copolymer poly(ethylene glycol)-*block*-poly(propylene glycol)-*block*-poly(ethylene glycol) ($PO_{20}EO_{70}PO_{20}$, M = 5800, Aldrich) and 0.03 mol of titanium isopropoxide (98%, ACROS) were dissolved in 30 mL of absolute ethanol. After the solution was vigorously stirred for 1 h, 0.003 mol of H_3PO_4 (85%, AJAX) was added into the solution. The resulting suspension was stirred for 30 min, followed by the addition of 40 mL of deionized water. The yellow powder was obtained after slow thorough vaporization of water and ethanol. The as-prepared samples were calcined at 400, 500, and 600 °C for 3 h with a heating rate of 5 °C/min, respectively. Pure mesoporous TiO_2 was also prepared without the addition of H_3PO_4.

X-ray powder diffraction (XRD) patterns were obtained using a Philips MPD 18801 diffractometer using Cu Kα radiation. Low-angle XRD patterns were recorded using a Bruker D8 Advance XRD diffractometer equipped with a Göbel mirror, using Cu Kα radiation.

Transmission electron microscopy (TEM) study was carried out on a Philips CM-120 electron microscopy instrument. The samples for TEM were prepared by dispersing the final powders in ethanol; the dispersion was then dropped on carbon−copper grids.

The nitrogen adsorption and desorption isotherms at 77 K were measured using a Micrometrics ASAP2010 system after samples were vacuum-dried at 200 °C overnight.

XPS measurements were performed in a VG Scientific ESCALAB Mark II spectrometer equipped with two ultra-high-vacuum (UHV) chambers. All binding energies were referenced to the C_{1s} peak at 284.8 eV of the surface adventitious carbon.

IR spectra on pellets of the samples mixed with KBr were recorded on a Nicolet Magna 560 FT-IR spectrometer at a resolution of 4 cm^{-1}. The concentrations of the samples were kept around 0.25−0.3%.

A Varian Cary 100 Scan UV−visible system equipped with a Labsphere diffuse reflectance accessory was used to obtain the reflectance spectra of the catalysts over a range of 200−600 nm. Labsphere USRS-99-010 was employed as a reflectance standard.

Isoelectric point measurements were carried out on a Brookhaven zeta plus analyzer. The suspension fluid was a 1 mM aqueous solution of potassium nitrate. The concentration of catalyst in the suspension was 1 mg mL^{-1}. The pH value of the suspension was adjusted using solution of 0.1 M nitric acid and 0.1 M potassium hydroxide.

Measurement of Photocatalytic Activity. The photocatalytic activity experiments on the mesoporous TiO_2 for the oxidation of *n*-pentane in air were performed at ambient temperature using a 3-L reactor. The photocatalysts were prepared by coating an aqueous suspension of titanium dioxide onto three dishes with a diameter of 5.0 cm. The weight of the photocatalyst used for each experiment was kept at 0.3 g. The dishes containing the photocatalyst were pretreated in an oven at 100 °C for 1 h and then cooled to room temperature before use.

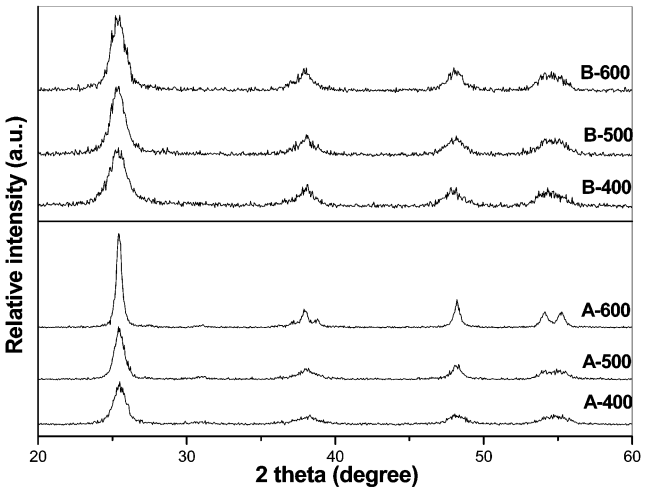

Figure 1. Wide-angle XRD patterns of MT and PMT calcined at different temperatures. A and B denote MT and PMT, respectively. The numbers following A and B denote the calcination temperatures.

Table 1. Summary of the Physicochemical Properties of Pure and Phosphated Mesoprous TiO_2

materials	calcination temperatures (°C)	crystalline size[a] (nm)	S_{BET}[b] (m^2/g)	mean pore size[c] (nm)	total volume[d] (cm^{-3}/g)
MT	400	9.0	137	7.4	0.44
	500	11.4	101	8.9	0.35
	600	21.8	54		0.23
PMT	400	6.0	301	3.4	0.58
	500	6.5	224	5.2	0.50
	600	6.9	168	7.4	0.47

[a] Calculated by the Scherrer equation. [b] BET surface area calculated from the linear part of the BET plot. [c] Estimated using the adsorption branch of the isotherm. [d] Single-point total pore volume of pores at $P/P_0 = 0.97$.

After the dishes coated with the photocatalysts were placed in the reactor, a small amount of *n*-pentane was injected into the reactor with a syringe. The reactor was connected to a pump and a dryer containing $CaCl_2$ for adjusting the starting concentration of *n*-pentane and controlling the initial humidity in the reactor. The analysis of *n*-pentane, carbon dioxide, and water vapor concentration in the reactor was performed with a Photoacoustic IR Multi-gas Monitor (INNOVA Air Tech Instruments Model 1312). The *n*-pentane vapor was allowed to reach adsorption equilibrium with the photocatalyst in the reactor prior to experimentation. The initial concentration of *n*-pentane after the adsorption equilibrium was 400 ppm, which remained constant until a 15-W 365-nm UV lamp (Cole-Parmer Instrument Co.) in the reactor was turned on. The initial concentration of water vapor was 1.20 ± 0.01 vol %, and the initial temperature was 25 ± 1 °C.

Results and Discussion

Effects of the Incorporation of Phosphorus on the Physicochemical Structure of Mesoporous TiO_2. Figure 1 shows the XRD patterns of MT and PMT calcined at different temperatures. The XRD pattern of pure anatase phase (JCPDS, No. 21-1272) is observed for all samples. Average crystalline sizes calculated from the broadening of the (101) XRD peak of anatase phase are 9.0 and 11.4 nm for MT calcined at 400 and 500 °C, respectively. Because of the growth of the quantum-sized grains, the crystalline size of MT increases to 21.8 nm after calcination at 600 °C (Table 1). In contrast with MT, the crystalline size of PMT does not change much

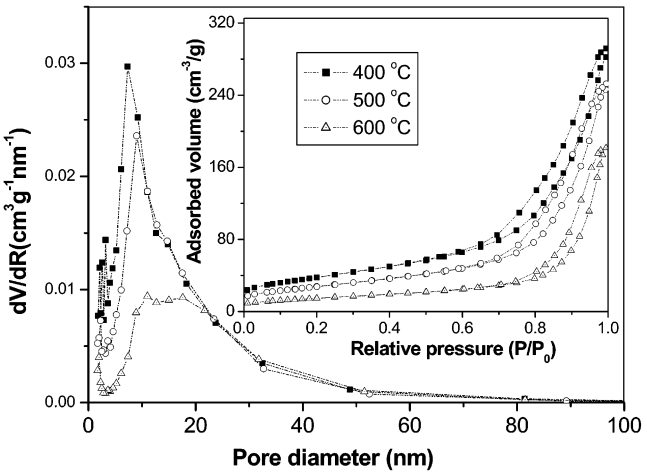

Figure 2. N_2 adsorption−desorption isotherms and Barret−Joyner−Halenda (BJH) pore size distribution plots (inset) of MT calcined at different temperatures.

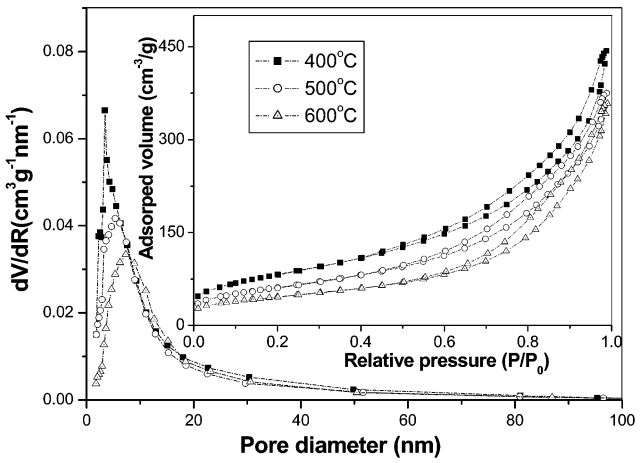

Figure 3. N_2 adsorption−desorption isotherms and Barret−Joyner−Halenda (BJH) pore size distribution plots (inset) of PMT calcined at different temperatures.

with calcination, indicating the inhibition of growth of anatase grains in PMT. The collapse of mesoporous framework of MT caused by the growth of TiO_2 grains in MT is clearly revealed by the low-angle XRD patterns shown in Figure S1 (Supporting Information). Both as-prepared MT and PMT possess one strong diffraction peak in the low-angle region, indicative of the presence of mesostructure. A single broad peak is observed on low-angle XRD patterns even for PMT calcined at 600 °C, suggesting the extremely high thermal stability of the PMT mesoporous framework. The mesostructure of MT is destroyed when treated at such a high temperature. It is known that wormhole-like mesostructures often display a single peak in low-angle XRD. The wormhole-like channels that are more or less regular in diameter are packed at random to form three-dimensional mesoporous structure. The regular separation between single-channel walls may have given rise to the single broad peak in the low-angle region. Similar disordered channels systems have been observed for disordered mesoporous TiO_2.[4]

The pore size distributions and N_2 adsorption−desorption isotherms (inset) of MT and PMT calcined at different temperatures are shown in Figures 2 and 3, respectively. Except for MT calcined at 600 °C, all the isotherms are type IV, which is characteristic of mesoporous materials. In all cases, the pore size distributions of PMT are narrower than that of MT. The difference is most significant for the samples calcined at 600 °C. The pore size distribution of MT becomes very broad, while PMT still maintains relatively narrow pore size distribution. The Brunauer−Emmett−Teller (BET) specific surface areas and pore volumes of MT and PMT are summarized in Table 1. Under all calcination conditions, the surface area of PMT is more than twice that of MT. The low surface area (54 m^2/g) of MT calcined at 600 °C confirms the complete destruction of the mesoporous structure. Obviously, the incorporation of phosphorus can stabilize the framework of mesoporous TiO_2.

TEM images of the as-prepared and calcined MT and PMT are presented in Figure 4. A wormhole-like mesostructure without long-range order can be observed on the edges of the TEM images of the as-prepared MT

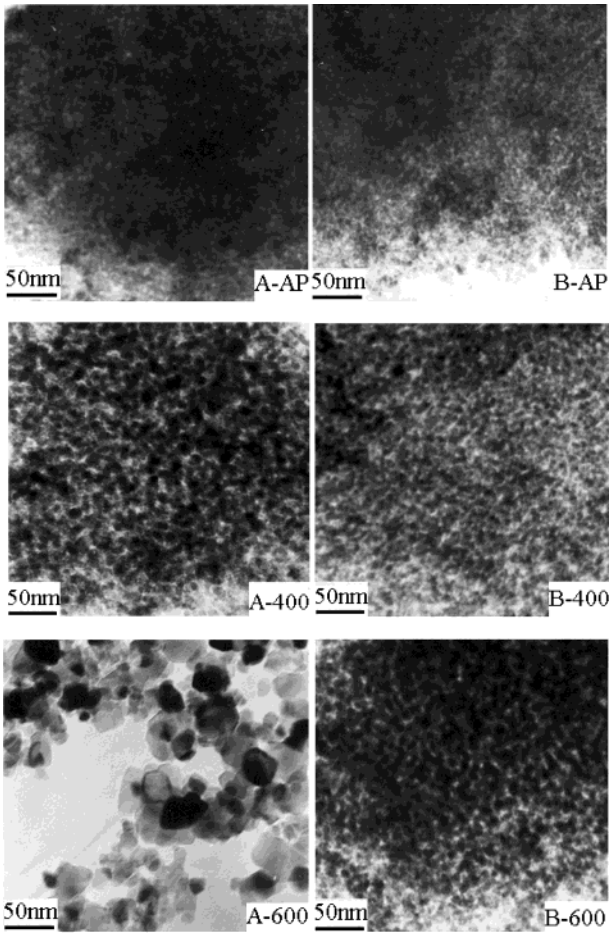

Figure 4. TEM images of as-prepared and calcined MT and PMT. A and B denote MT and PMT, respectively. AP following A and B denote as-prepared sample. The numbers following A and B denote the calcination temperatures.

and PMT. The wormhole-like mesoporous structure is also found in the TEM images of both MT and PMT after calcination at 400 °C. However, the mesoporous structure is completely destroyed for MT after calcination at 600 °C. This is consistent with the low-angle XRD results. The crystalline sizes of the calcined MT and PMT estimated from the TEM images are in good

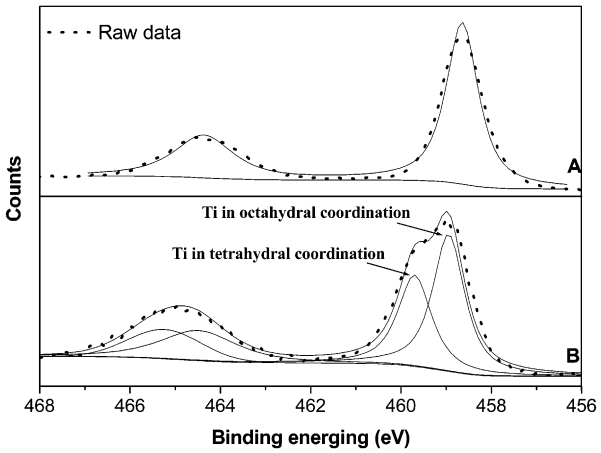

Figure 5. High-resolution XPS spectra of the Ti 2p region taken on the surface of MT and PMT calcined at 600 °C. A and B denote MT and PMT, respectively.

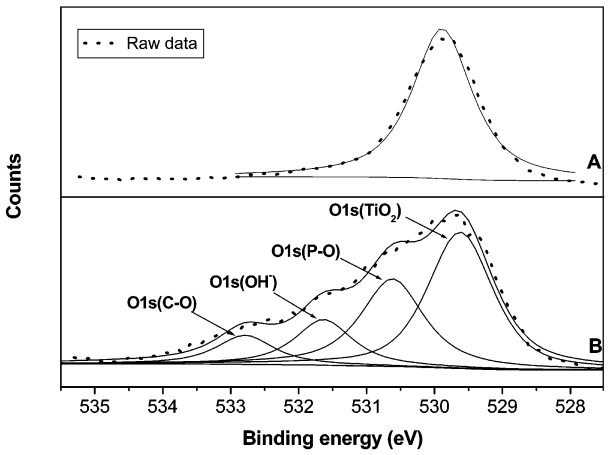

Figure 6. High-resolution XPS spectra of the O 1s region taken on the surface of MT and PMT calcined at 600 °C. A and B denote MT and PMT, respectively.

agreement with that calculated by using the Scherrer equation.

Figure 5 shows the high-resolution XPS spectra of Ti taken on the surface of MT and PMT calcined at 600 °C. Ti $2p_{3/2}$ in MT can be fitted as one peak at 458.7 eV, indicating that Ti ions are in an octahedral environment. For Ti in PMT, the broad Ti $2p_{3/2}$ consists of two peaks at 458.9 and 459.7 eV with an atomic ratio of about 59 to 41, respectively. This implies the two different chemical environments of Ti ions exist in the calcined PMT structure. The first Ti ions can be assigned to an octahedral coordination with oxygen, and the second Ti ions are in a tetrahedral environment.[18] The P 2p binding energy of PMT is observed at 133.8 eV. It is unlikely that Ti−P bonds are present in the calicned PMT since the characteristic binding energy of Ti in TiP at 128.6 eV was not observed.[19] The binding energy of 133.8 eV suggests that phosphorus in the calcined PMT exists in a pentavalent-oxidation state (P^{5+}).[20] Figure 6 shows the high-resolution XPS spectra of the O 1s region taken on the surface of MT and PMT calcined at 600 °C. The O 1s region of the calcined MT is composed of a single peak at 529.8 eV, corresponding to the Ti−O in TiO_2. However, the broad O 1s region of the calcined PMT can be fitted by four peaks, which are Ti−O in TiO_2, P−O bonds, hydroxyl groups, and C−O bonds, respectively. The binding energy of the Ti−O in TiO_2 is 529.6 eV with 45.4% in contribution, and the binding energy of the P−O is 530.6 eV with 30.8% in contribution. For the hydroxyl groups and the C−O bonds, the binding energies are 531.6 and 532.8 eV with 14.6% and 9.2% in contribution, respectively.

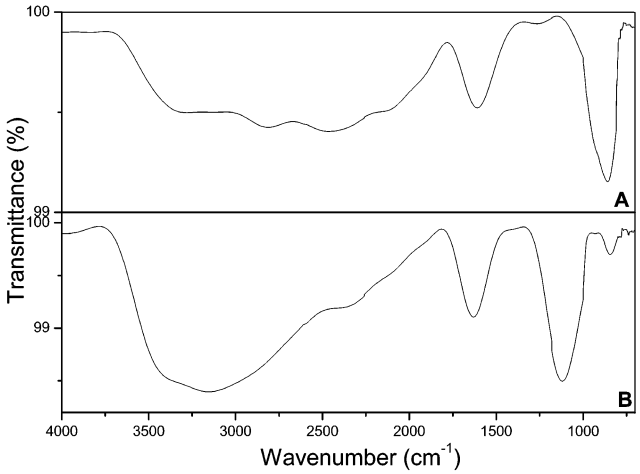

Figure 7. FT-IR spectra of MT and PMT calcined at 600 °C. A and B denote MT and PMT, respectively.

The FT-IR spectra of MT and PMT calcined at 600 °C are shown in Figure 7. It is believed that the broad peak at 3400 and the peak at 1650 cm^{-1} correspond to the surface-adsorbed water and hydroxyl groups.[21] Obviously, the calcined PMT has more surface-adsorbed water and hydroxyl groups than the calcined MT, which confirms the XPS results. This can be attributed to the larger surface area of the calcined PMT and the presence of Ti ions in a tetrahedral coordination in the calcined PMT. Ti ions in a tetrahedral coordination are more effective in adsorbing water.[22] A broad absorption peak at 963−1288 cm^{-1} is observed on the IR spectra of PMT but absent for the calcined MT. The peaks in this range are often the characteristic frequencies of PO_4^{3-}. However, the absence of phosphoryl (P═O) peaks at 1300−1400 cm^{-1} does not support that presence of PO_4^{3-} in PMT.[23] Therefore, we believe that the phosphorus exists as Ti−O−P in the calcined PMT. The peak at 850 cm^{-1} corresponds to the Ti−O−Ti stretching vibration of Ti ions in an octahedral coordination.[24] The drastic decrease in the intensity of this peak in the spectrum of PMT confirms the diminishing octahedral coordination of the Ti ions. It was known that the P−O−P deformation vibration can produce a peak at about 750 cm^{-1} in the IR spectrum.[23,24] As no distinct peaks can be observed over the range of 400−800 cm^{-1}, P−O−P is absent in the calcined PMT.[25] Therefore, we conclude that the phosphorus is incorporated into the framework of mesoporous TiO_2 by forming Ti−O−P

(18) Alfaya, A. A. S.; Gushikem, Y. *Chem. Mater.* **1998**, *10*, 909.
(19) Baunack, S.; Oswald, S.; Scharnweber, D. *Surf. Interface Anal.* **1998**, *26*, 471.
(20) Splinter, S. J.; Rofagha, R.; Mcintyre, N. S.; Erb, U. *Surf. Interface Anal.* **1996**, *24*, 81.
(21) Ding, Z.; Lu, G. Q.; Greenfield, P. F. *J. Phys. Chem. B* **2000**, *104*, 4815.
(22) Jones, P.; Hockey, J. A. *Trans. Faraday Soc.* **1971**, *67*, 2679.
(23) Bhaumik, A.; Inagaki, S. *J. Am. Chem. Soc.* **2001**, *123*, 691.
(24) Sigaev, V. N.; Pernice, P.; Aronne, A.; Akimova, O. V.; Stefanovich, S. Y.; Scaglione, A. *J. Non-Cryst. Solids* **1990**, *126*, 202.

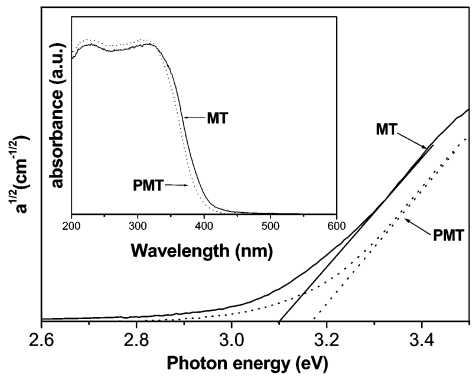

Figure 8. Plots of $a^{1/2}$ versus photon energy and UV−vis absorbance spectra (inset) of MT and PMT calcined at 600 °C. *a* is the absorption coefficient. Solid line (—) and dotted line (···) denote MT and PMT, respectively.

bonds. It does not exist as PO_4^{3-} or polyphosphoric acid attached to the TiO_2 surface.

Because of the quantum-size effect, the UV−vis absorption band edge is a strong function of titania cluster size for diameters <10 nm.[26,27] Figure 8 shows that the UV−vis spectra of PMT calcined at 600 °C is blue-shifted by several nanometers in comparison with that of MT calcined at 600 °C. This indicates that the band gap of the calcined PMT is larger than that of the calcined MT. The band gaps of the calcined PMT and MT are estimated to be 3.17 and 3.10 eV from the $a^{1/2}$ versus photon energy plots, respectively.[27]

The isoelectric points of the calicned PMT and MT are 5.8 and 5.4, respectively (Supporting Information). The low isoelectric point in terms of pH value means a higher concentration of hydroxide groups on the surface of the catalyst.[7] Thus, it can be concluded that there are more hydroxide groups on the surface of PMT than that of MT. This is consistent with XPS and FT-IR results. This higher surface acidity of the calcined PMT can be attributed to the presence of Ti ions in a tetrahedral coordination, which can act as Lewis acid sites.[28] These Lewis acid sites can easily adsorb oxygen and water molecules.[22,29]

Possible Model of the Framework of Calcined Phosphated Mesoporous TiO_2 and the Stabilization Mechanism of Mesopores. It is well-known that a large amount of uncondensed Ti−OH exists on the surface of the as-prepared amorphous mesoporous TiO_2. During calcination, the rapid reactions between the uncondensed Ti−OH would cause the walls of mesoporous TiO_2 to collapse. This is why pure mesoporous TiO_2 has a relatively poor thermal stability. It has been reported that post-treatment with H_3PO_4 would improve the stability of mesoporous Al−MCM-41 and zirconia.[15,17] Reactions between phosphoric acid and uncondensed Ti−OH in the as-prepared PMT may result in more completely condensed walls, which effectively prevent the collapse of the mesoporous structure during calcination. It has also been reported that when triblock copolymer was used as a structure-directing agent, the calcined mesoporous TiO_2 exhibited a robust inorganic framework with thick channel walls. These walls consist of amorphous TiO_2 with embedded semicrystalline anatase of only about 3 nm in size.[30,31] Since the Ti ions in mesoporous titanium phosphate are mainly in a tetrahedral environment,[22] we believe that our calcined PMT contains titanium phosphate. As no peaks corresponding to titanium phosphate were observed in the XRD patterns of PMT even after calcination at 600 °C, the titanium phosphate should be amorphous in nature. On the basis of the results of TEM images, XPS analysis, and FT-IR spectra, a model of the framework of the calcined PMT is proposed. It is comprised of amorphous titanium phosphate embedded with well-crystallized anatase of 6−7 nm in size. The presence of an amorphous titanium phosphate wall between the TiO_2 crystalline grains is crucial in the stabilization of PMT. It acts as a diffusion barrier to inhibit TiO_2 crystal growth during calcination, leading to high thermal stability for PMT. In summary, the stabilization of mesoporous TiO_2 framework by the direct incorporation of phosphorus from H_3PO_4 can be attributed to two reasons: the more complete condensation of surface Ti−OH in the as-prepared sample and the inhibition of crystalline grain growth of the embedded anatase TiO_2 by the interspersed amorphous titanium phosphate matrix that provides dissimilar boundaries during calcination.[32,33]

XPS analysis shows that the atomic percentage of Ti ions in a tetrahedral coordination in the calcined PMT is about 41%, while the overall atomic ratio of P to Ti is ≈14%. We think that some of the Ti ions in a tetrahedral coordination may also come from the anatase in the calcined PMT. It is known that Ti ions on the external surface of TiO_2 are partly four- or five-coordinated, especially in particles with size smaller than 20 nm.[29] These unsaturated-coordinated species may exhibit different reactivities and surface properties.[34] Therefore, photocatalytic activity of the calcined PMT is worth exploring.

Photocatalytic Activity Studies. The results of photocatalytic degradation of *n*-pentane over the calcined MT and PMT are presented in Figure 9. The photocatalytic activity of commercial nonporous photocatalyst P25 was measured under identical conditions for comparison. During the degradation reaction of *n*-pentane, it was observed that the degradation of each ppm of *n*-pentane could produce 5 ppm CO_2 in the reactor.[27] Therefore, we believe that *n*-pentane is decomposed completely into CO_2 in our system. Both MT and PMT show better photocatalytic activities than the commercial photocatalyst P25. This can be attributed to their high surface area and the facile diffusion of

(25) Jimenez-Jimenez, J.; Maireles-Torres, P.; Olivera-Pastor, P.; Rodriguez-Castellon, E.; Jimenez-Lopez, A.; Jones, D. J.; Roziere, J. *Adv. Mater.* **1998**, *10*, 812.
(26) Zhang, Q. H.; Gao, L.; Guo, J. H. *Appl. Catal., B* **2000**, *26*, 207. Hoffmann, M. R.; Martin, S. T.; Choi, W. Y.; Bahnemann, D. W. *Chem. Rev.* **1995**, *95*, 69.
(27) Yu, J. C.; Zhang, L. Z.; Yu, J. G. *Chem. Mater.* **2002**, *14*, 4647.
(28) Makarova, O. V.; Dakka, J.; Shedon, R. A.; Tsyganenko A. A. *Stud. Surf. Sci. Catal.* **1995**, *94*, 163.
(29) Suda, Y.; Morimoto, T. *Langmuir* **1987**, *3*, 786. Rajh, T.; Nedeljkovic, J. M.; Chen, L. X.; Poluektov, O.; Thurnauer, M. C. *J. Phys. Chem. B* **1999**, *103*, 3515.
(30) Yang, P. D.; Zhao, D. Y.; Margolese, D. I.; Chmelka, B. F.; Stucky, G. D. *Chem. Mater.* **1999**, *11*, 2813.
(31) Yang, P. D.; Zhao, D. Y.; Margolese, D. I.; Chmelka, B. F.; Stucky, G. D. *Nature* **1998**, *396*, 152.
(32) Yu, J. C.; Lin, J.; Kwok, R. W. M. *J. Phys. Chem. B* **1998**, *102*, 5094.
(33) Fu, X.; Clark, L. A.; Yang, Q.; Anderson, M. A. *Environ. Sci. Technol.* **1996**, *30*, 647.
(34) Oliver, P. M.; Watson, G. W.; Kelsey, E. T.; Parker, S. C. *J. Mater. Chem.* **1997**, *7*, 563.

reactants in the wormhole-like mesopores.[4]

It is interesting to note that the calcined PMT has better photocatalytic activity than the calcined MT. Stone and Davis[10] used the dodecyl phosphate surfactant as a template to synthesize a mesoporous titania with an extremely large surface area. However, they found that phosphorus from the template was bound so strongly to the molecular sieve that it could not be removed completely by either calcination or solvent extraction. They attributed the low photocatalytic activities of their mesoporous titania samples to a high surface concentration of defects and/or the poisoning of catalytic surface sites by the phosphorus remaining from the surfactant. Putman et al.[35] also synthesized titanium dioxide-surfactant mesophases using a similar procedure. They found that potassium titanium oxyphosphate ($KPOTiO_4$), potassium titanium phosphate ($KTi_2(PO_4)_3$), and anatase TiO_2 were together in the sample calcined at 500 °C for 24 h. Since our calcined PMT containing amorphous titanium phosphate and well-crystallized anatase TiO_2 shows high photocatalytic activity, we believe the poor photocatalytic activity of mesoporous TiO_2 synthesized with phosphate-containing surfactants is not caused by the poisoning of catalytic surface sites by the phosphorus from the surfactant. In addition, our preliminary results indicate that the photocatalytic activity of phosphated mesoporous TiO_2 is affected by the proportion of the titanium phosphate phase present in the material. Further studies are necessary to clarify the effects of the content of titanium phosphate on the photocatalytic activity.

The high photocatalytic activity of the calcined PMT can be explained by the band gap, surface area, and coordination of Ti ions. It is commonly accepted that a larger band gap corresponds to a more powerful redox ability.[36] Since the calcined PMT has a larger band gap than the calcined MT, its oxidizing ability should be stronger. Furthermore, the oxidative reaction of *n*-pentane is believed to be initiated by OH radicals. In the presence of O_2, the OH radicals are formed in the following reactions:[37]

$$TiO_2 \rightarrow h^+ + e^- \quad (1)$$

$$e^- + O_2 \rightarrow O_2^- \quad (2)$$

$$O_2^- + 2H^+ + e^- \rightarrow H_2O_2 \quad (3)$$

$$H_2O_2 + O_2 \rightarrow {}^\bullet OH + OH^- + O_2 \quad (4)$$

$$h^+ + H_2O \rightarrow {}^\bullet OH + H^+ \quad (5)$$

The incorporation of phosphorus enhances the surface area of the calcined catalysts by more than 100 m^2/g (Table 1). Mesoporous TiO_2 of larger surface area can offer more active sites to adsorb water and hydroxyl groups. Meanwhile, Ti ions in tetrahedral coordination can provide additional surface hydroxyl groups by adsorbing water in air.[27] These two factors are thought to enhance the surface-adsorbed water and hydroxyl groups on the calcined PMT, which is confirmed by the lower isoelectric point of PMT than that of MT. According to eq 5, the surface-adsorbed water and hydroxyl groups can react with photoexcited holes on the catalyst surface and produce hydroxyl radicals, which are powerful oxidants in degrading organics.[7]

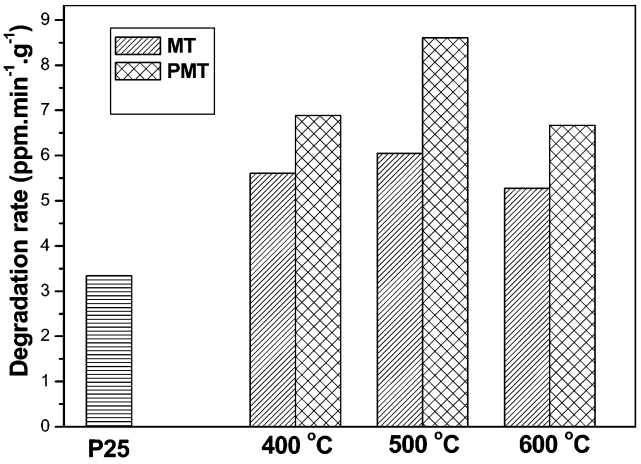

Figure 9. Photocatalytic activities of MT and PMT calcined at different temperatures.

Yamashita et. al [37] reported that tetrahedral titanium oxide moieties on the surface layer of the silica glass could be responsible for the high photocatalytic activity. However, the authors did not provide explanation to the high activity. We believe that the Ti ions in tetrahedral coordination offer a number of benefits. These tetrahedrally coordinated Ti ions can adsorb water and oxygen in air to produce more hydroxyl groups on the surface of TiO_2. Moreover, the adsorbed water and oxygen by the Ti ions in tetrahedral coordination can stabilize the photoexcited hole and electron pairs.[38] This would slow the rate of e^-—h^+ recombination and increase the photocatalytic activity.

Conclusions

Direct incorporation of phosphorus into the inorganic framework of mesoporous TiO_2 from H_3PO_4 can stabilize the mesoporous structure of TiO_2. The grain growth is inhibited and the surface area increases significantly. On the basis of TEM images, XPS analysis, and FT-IR spectra, we propose that the calcined phosphated mesoporous TiO_2 is comprised of amorphous titanium phosphate with embedded crystalline anatase of 6—7 nm in size. This is different from the framework of pure mesoporous TiO_2. The stabilization of the phosphated mesoporous TiO_2 framework can be attributed to two reasons: the more complete condensation between surface Ti—OH in the as-prepared sample and the inhibition of crystalline grain growth of the embedded anatase TiO_2 during the calcination.

The calcined phosphated mesoporous TiO_2 exhibits higher photocatalytic activity than both the calcined pure mesoprous TiO_2 and the commercial nonporous photocatalyst P25. We conclude that the high photocatalytic activity of the calcined phosphated mesoporous TiO_2 is related to its extended band gap energy, larger

(35) Putnam, R. L.; Nakagawa, N.; McGrath, K. M.; Yao, N.; Aksay, I. A.; Gruner, S. M.; Navrotsky, A. *Chem. Mater.* **1997**, *9*, 2690.
(36) Lin, J.; Yu, J. C.; Lo, D.; Lam, S. K. *J. Catal.* **1999**, *183*, 368.
(37) Yamashita, H.; Honda, M.; Harada, M.; Ichihashi, Y.; Anpo, M.; Hirao, T.; Itoh, N.; Iwamoto, N. *J. Phys. Chem. B* **1998**, *102*, 10707.
(38) Tsai, S. J.; Cheng, S. *Catal. Today* **1997**, *33*, 227.

surface area, and the existence of Ti ions in a tetrahedral coordination. The causes for the photocatalytic activity enhancement with Ti ions in a tetrahedral coordination are also discussed.

Acknowledgment. The work described in this paper was partially supported by a grant from the National Natural Science Foundation of China and Research Grants Council of the Hong Kong Special Administrative Region, China (Project No. N-CUHK 433/00).

Supporting Information Available: Low-angle XRD patterns and zeta potential−pH value plots of MT and PMT (PDF). This material is available free of charge via the Internet at http://pubs.acs.org.

CM0340781